The Journal of Experimental Biology 216, 524-534

doi:10.1242/jeb.079095

RESEARCH ARTICLE

Lobula-specific visual projection neurons are involved in perception of motion-defined second-order motion in *Drosophila*

Xiaonan Zhang[1,3,*], He Liu[2,3,*], Zhengchang Lei[2,3], Zhihua Wu[1,†] and Aike Guo[1,2,†]

[1]State Key Laboratory of Brain and Cognitive Science, Institute of Biophysics, Chinese Academy of Sciences (CAS), Beijing 100101, China, [2]Institute of Neuroscience, State Key Laboratory of Neuroscience, Shanghai Institutes for Biological Sciences, CAS, Shanghai 200031, China and [3]Graduate University of CAS, Beijing 100049, China

*These authors contributed equally to this work

†Authors for correspondence (wuzh@moon.ibp.ac.cn; akguo@ion.ac.cn)

SUMMARY

A wide variety of animal species including humans and fruit flies see second-order motion although they lack coherent spatiotemporal correlations in luminance. Recent electrophysiological recordings, together with intensive psychophysical studies, are bringing to light the neural underpinnings of second-order motion perception in mammals. However, where and how the higher-order motion signals are processed in the fly brain is poorly understood. Using the rich genetic tools available in *Drosophila* and examining optomotor responses in fruit flies to several stimuli, we revealed that two lobula-specific visual projection neurons, specifically connecting the lobula and the central brain, are involved in the perception of motion-defined second-order motion, independent of whether the second-order feature is moving perpendicular or opposite to the local first-order motion. By contrast, blocking these neurons has no effect on first-order and flicker-defined second-order stimuli in terms of response delay. Our results suggest that visual neuropils deep in the optic lobe and the central brain, whose functional roles in motion processing were previously unclear, may be specifically required for motion-defined motion processing.

Supplementary material available online at http://jeb.biologists.org/cgi/content/full/216/3/524/DC1

Key words: motion perception, non-Fourier motion, *Drosophila*, optomotor response, lobula, visual projection neuron.

Received 13 August 2012; Accepted 1 October 2012

INTRODUCTION

Motion perception is vital to the survival of visual animals. In addition to first-order (Fourier) motion, second-order (non-Fourier) motion stimuli are visible to a wide variety of animal species including humans, zebrafish and flies (Lu and Sperling, 1995; Baker, 1999; Orger et al., 2000; Theobald et al., 2008). First-order motion is formed by luminance modulation across space and time, whereas second-order stimuli have the same luminance everywhere but different local features (such as contrast, flicker or texture) from the background. For example, a dark vertical bar moving against a random-dot background consisting of black and white dots is one type of first-order motion stimulus. If the vertical bar is removed and only the local contrast of the random-dot background pattern is manipulated, motion can also be perceived. For instance, by reversing the contrast of a single column of the random-dot background each time and shifting the locations of the changes to the right by one dot between each frame, we can clearly perceive horizontal motion although there is no coherent dot motion at all. The illusion of the horizontal motion gives one example of flicker-defined second-order motion. Theoretically, first- but not second-order motion stimuli can be detected by the correlation-type elementary movement detector (Borst and Egelhaaf, 1989). Previous studies have investigated the neuronal circuit mechanisms underlying second-order stimuli processing in mammals (Demb et al., 2001; Rosenberg and Issa, 2011); however, where and how the higher-order motion signals are processed in the fly brain is poorly understood.

Fly vision relies mainly on motion perception. Fruit flies see not only flicker-defined second-order motion but also theta motion (Theobald et al., 2008; Theobald et al., 2010). Unlike other second-order stimuli, which are defined by modulations of higher-order features, such as local flicker, contrast or texture, theta motion (Quenzer and Zanker, 1991) is the displacement of an object whose internal texture (dots in our case) moves coherently in the opposite direction to the object. It is therefore a kind of motion-defined second-order motion (MDSM). As one of the best-studied neuropils in the fly optic lobe, the lobula plate is commonly thought to be responsible for Fourier motion processing (Borst et al., 2010; Joesch et al., 2008), but the neural correlates of second-order motion detection remain open in flies. Meanwhile, little is known about the role and function of the lobula, the lobula plate's neighbor in the third optic ganglion, in motion signal processing. Anatomical evidence has predicted that the lobula is mainly sensitive to object features, such as orientation, texture and color (reviewed by Douglass and Strausfeld, 2003). The identification of a considerable number of mutual projections between the lobula, lobula plate and the central brain suggests that motion information may need to be transmitted between these brain regions for further integration and computation (Douglass and Strausfeld, 2003; Otsuna and Ito, 2006; Fischbach and Dittrich, 1989; Strausfeld, 1991). In this paper we investigated whether the lobula-specific visual projection neurons (VPNs) that specifically connect the lobula and the central brain are required for second-order motion processing. By manipulating two VPNs (LT10 and LT11) in *Drosophila* (Otsuna and Ito, 2006)

and examining the behavioral responses to several types of first- and second-order stimuli, we found that LT10 and LT11 are involved in the processing of MDSM but may be dispensable for the first-order and flicker-defined second-order stimuli. To our knowledge, the results are the first evidence showing the involvement of the lobula in second-order motion processing to date.

MATERIALS AND METHODS

Flies and preparation

Female flies (*Drosophila melanogaster* Meigen 1830) aged 3–5 days post-eclosion were used in all experiments. Wild-type strain *Canton-S* (CS) and the following mutants were used: NP5006, NP7121, NP6099, NP1047 and NP1035 (NP Consortium, Kyoto Stock Center, Ukyo-ku, Kyoto, Japan). The mutants were used as Gal4 lines to label LT10 and LT11; Fig. 1C and supplementary material Fig. S1A show examples of such response traces.

Flies were cultured at 25°C and 60% humidity on standard medium under a 12 h:12 h light:dark cycle (Guo et al., 1996). On the day before behavioral experiments flies were briefly immobilized by cold anesthesia. A tiny triangle-shaped hook 0.05 mm in diameter was glued to the dorsal thorax and head of each fly. Flies were kept individually in small chambers and allowed to recover overnight by feeding with sucrose solution.

Visual stimuli

The tethered flies were suspended from a torque meter in front of an LCD screen (ViewSonic, VX2268wm, 120 Hz, Walnut, CA, USA), on which the visual stimuli were presented (Fig. 1A). The distance between the LCD monitor and the fly was 45 mm. The stimulus was programmed by Visual Studio (Microsoft, Redmond, WA, USA) and was generated at a rate of 40 frames s^{-1}. The mean luminance of the stimulus patterns was 97 Cd m^{-2}, and the contrast was nearly 100% under the dark experimental conditions used here. Several types of motion patterns were used in experiments: first-order or Fourier motion, two kinds of flicker-defined second-order motion, theta motion (Quenzer and Zanker, 1991), and two kinds of theta-like motion (supplementary material Movie 1). Theta motion and theta-like motion patterns are types of second-order motion defined by their internal motion modulation. Except for two kinds of theta-like motion, all other stimuli consisted of a random-dot background and a superimposed vertical figure with the same texture as the background. The background consisted of 128×75 black and white dots and corresponded to a visual angle of 142×120 deg as seen by the fly. Each dot consisted of 8×8 pixels and was equivalent to a visual angle of approximately 1.5 deg. The vertical figure was 24 dots wide. Because the figure had the same texture as the static background, it was visible as a distinct object only when it was moving relative to the static background.

Each type of motion stimulus lasted 20 s, during which the position of the vertical figure oscillated uniformly and horizontally about phase 0 deg at 0.25 Hz with an amplitude of ±58 deg for five cycles. Phase 0 deg was defined as the frontal midline of the test fly. In terms of speed, the figure moved at 40 dots s^{-1}, which was equivalent to 80 deg s^{-1} in the phase 0 deg direction of view. A Fourier bar was generated by making the dots of the figure move coherently with the figure position. To produce theta motion, the dots within the figure, also called theta object or theta bar, were made to move in the opposite direction to the figure itself (Quenzer and Zanker, 1991). Two kinds of flicker-defined motion stimuli were used: a flicker bar motion designed by simply reversing the contrast of all the dots within the figure when the figure was moving, and a flicker border motion that was generated by setting the reverse speed of dots within the theta object to zero. Three more theta stimuli were generated by just changing the speed of internal dots to –10, –20 and –80 dots s^{-1}; the negative sign means that the internal dots were moving in the opposite direction to the theta bar. Similar to the metrical method used by Theobald et al. (Theobald et al., 2010), a dimensionless ratio of the internal dot speed to the theta bar speed was employed. Thus the ratio ranges from +1 to –2, representing a change in internal dot motion from completely coherent with (Fourier stimulus) to opposing to the external bar (theta motion with internal dot speed of –80 dots s^{-1}).

Theta-like motion, which did not require a superimposed vertical figure, was generated on the same random-dot background as that used for theta motion. Within a 24 dot wide figure, all dots were displaced coherently and vertically at a constant speed of 20 dots s^{-1}. When one row of moving dots disappeared at the border of the figure in the direction of the motion, a row of newly generated dots appeared at the other figure border. Simultaneously, the position of the figure oscillated uniformly and horizontally for five cycles with the same frequency and amplitude as the theta object. The stimulus duration was 20 s, during which the direction of the inside dots was always upward or downward for simplification. Such a design gives the illusion of horizontal motion, although there is no first-order motion component in the horizontal direction: the individual dots did not move sideways but only up or down. Theta-like motion can be regarded as a simpler version of the second-order motion used previously (Roeser and Baier, 2003).

Stimuli were presented in a random order with a 10 s interval of noise distraction, in which dots from the random-dot background jumped around erratically. All tested flies were naive. Each stimulus was presented to each individual fly only once. The optomotor response trace was recorded at a sample frequency of 40 Hz. Flies that paused during tracking of a given stimulus were excluded from the results.

Response measurements

The torque meter (Götz, 1964) was used to measure the optomotor responses of yaw torque about the vertical axis of the fly (Heisenberg and Wolf, 1979) which were blocked and highlighted by crossing these Gal4 lines with the upstream activating sequence (UAS) TNT strain (Sweeney et al., 1995) and the UAS-mCD8-GFP strain, respectively. However, the torque meter is not useful for probing pitch torque when we needed to test the fly's optomotor responses to vertically moving stimuli. Therefore, we developed an acoustic flight simulator (AFS) based on Götz's wing beat processor (WBP) (Götz, 1987) (supplementary material Fig. S2). The AFS monitors the wing strokes by recording the wing's beating sound instead of measuring its shadow area casted on a photodetector in the WBP (Götz, 1987). The beating sound is picked up by a pair of tiny microphones at constant angle and distance from the wings. To record the maximum signal, the microphones were placed posterolateral to the fly at a distance less than 1 mm from the wings. In each flapping cycle, the downstroke and the upstroke of a wing produce a major and minor peak in sound signal, respectively. This 'dual-peak' waveform is similar to that detected by the WBP (Götz, 1987). The beating sound signal is firstly amplified and filtered (bandpass filter, 2 Hz to ~5 kHz) and then processed by a peak detection circuit to calculate the amplitude of the dual-peak wave, through which the wing beat strength (WBS) is recorded as the output signal. The AFS records the WBS traces of both wings [left (L) and right (R)] in real-time. Because ΔWBS is proportional to yaw torque (Götz, 1987; Tammero et al., 2004), the L–R WBS signal is used to measure the horizontal turning of the flight. It is coincident

with that measured by the torque meter (supplementary material Fig. S2A). The L+R WBS signal reflects the pitch behavior and is used to measure the fly's response to vertical motion stimuli (supplementary material Fig. S2B,C).

Data analysis

Cross-correlation analysis between the response traces and the time course of the bar position with a frequency of 0.25 Hz was performed. Because cross-correlation analysis is highly sensitive to between-trial variation, as pointed out by Theobald et al. (Theobald et al., 2010), the analysis was mainly performed on the average response traces. To investigate the within-genotype variability in response behavior, individual fly's response trace-based analysis was also performed as specified in the Results.

The optomotor response traces of individual flies were normalized prior to being averaged for cross-correlation analysis, and the lag range over which the cross-correlation coefficient was computed was set as [–2000 ms, +2000 ms]. The maximal cross-correlation coefficient (MCC) and the corresponding time lag were used as two indices for describing the response trace's similarity or fidelity to the stimulus and the response delay, respectively. We also tried to compute the cross-correlation by directly averaging individual response traces over flies without normalization. Without normalization, the MCC and lag displayed slight differences from those obtained by applying normalization, and only the former approach was adopted in the present study.

Immunohistochemistry and confocal microscopy

Brains of female flies with Gal4-driven green fluorescent protein (GFP) expression were dissected 3 to 6 days after eclosion. After fixation in 2% paraformaldehyde for 1 h at room temperature, the brains were washed three times in 0.3% PBST (phosphate-buffered saline, pH 7.4 with 1% Triton X-100) for a total of 60 min. The brains were next incubated in 5% normal goat serum (Invitrogen, PCN5000, Carlsbad, CA, USA) for 1 h at room temperature and then in primary antibodies (1:100) overnight at 4°C. The primary antibody was nc82 (Developmental Studies Hybridoma Bank, Iowa, IA, USA). Samples were subsequently washed with PBST at least three times for a total of 1 h and incubated with a secondary antibody (1:100) overnight at 4°C. The secondary antibody (Alexa Fluor 568 goat anti-mouse IgG, A11031; Molecular Probes, Invitrogen) was removed by washing samples three times for a total of 1 h.

Serial optical sections were taken by a Nikon confocal microscope (A1R on FN1, Nikon, Chiyoda-ku, Tokyo, Japan) and a water-immersion 40× objective (NIR Apo 40×/0.80 w, Nikon). Sections were taken at 1.5 µm intervals at a resolution of 512×512 pixels. The size, contrast and brightness of the serial sections were adjusted with ImageJ (National Institutes of Health, Bethesda, MD, USA).

RESULTS

Using the experimental setup shown in Fig. 1A, we investigated whether the lobula-specific VPNs are involved in second-order motion processing. These VPNs have been anatomically described in several fly species (Douglass and Strausfeld, 2003; Otsuna and Ito, 2006; Fischbach and Dittrich, 1989). Of the 14 pathways identified in *Drosophila* (Otsuna and Ito, 2006), we were interested in VPNs that have tangential or tree-like arborizations and that can be unequivocally labeled by Gal4 strains. The former criterion distinguishes VPNs that may possess large receptive fields. Tangential or tree-type neurons LT10 and LT11 were chosen for study (Fig. 1B). LT10 is centripetal and some presynaptic sites of LT11 are found in the ventrolateral protocerebrum, implying that the two types of neurons may send visual information to the central brain for further computation (Otsuna and Ito, 2006). LT10 is labeled by Gal4 strains NP5006 and NP7121, and LT11 is labeled by NP6099 and NP1047. NP1035 labels both LT10 and LT11 (Otsuna and Ito, 2006). To examine the effect of blocking LT10 and/or LT11 on motion perception, the VPNs LT10 and/or LT11 were blocked by crossing these Gal4 lines with a UAS-TNT strain (Sweeney et al., 1995), which eliminates the synaptic transmission by cleaving synaptobrevin (a synaptic vesicle membrane protein). The heterozygotes NP5006/+, NP7121/+, NP6099/+, NP1047/+, NP1035/+ and TNT/+ were generated by crossing Gal4 or UAS lines with wild-type strain CS as controls.

Blocking lobula-specific VPNs LT10 and LT11 reduces response amplitude to both first- and second-order motion stimuli

Six types of motion pattern (Fig. 1C, left column; supplementary material Movie 1) were presented to flies in which LT10 and/or LT11 were blocked, their controls and the CS flies. The Fourier stimulus is first-order bar motion. Flicker and flicker border stimuli are flicker-defined second-order motion, but they differ in terms of the dynamic characteristics within the moving bar: in the flicker stimulus, all the dots inside the flicker bar flickered as the bar moved; whereas in the flicker border stimulus, the area marked by two flickering borders was static. The other three patterns are MDSM defined by their internal motion modulation. The internal first-order components of the theta and theta-like motion were directionally opposite and perpendicular to their second-order moving features, respectively. To remove systematic bias from unidirectional movement within the theta-like object, two kinds of theta-like motion stimuli, including the one shown in Fig. 1C and another in which the inside dots moving always upward, were presented in a random order with equal probability (supplementary material Movie 1). The theta-like border motion was similar to the theta-like stimulus, except that the dots inside the theta-like object were stationary and only its two borders, each one column of dots wide, moved.

The mean optomotor response traces to each stimulus of the CS flies and three blocking strains are shown in Fig. 1C and those of their heterozygous Gal4 lines and UAS-TNT control are shown in supplementary material Fig. S1. To obtain average traces, optomotor response traces to each motion stimulus were pooled across individual flies of each strain and averaged without prior normalization. In addition to Fourier, flicker, flicker border and theta motion, which were previously found to be visible to CS flies (Theobald et al., 2008; Theobald et al., 2010), theta-like and theta-like border also evoked robust steering response in the CS strain. These results indicate that MDSM is visible to fruit flies, independent of whether the second-order feature is moving perpendicular or opposite to the local first-order motion. Trace amplitude-based visual inspection suggests that strains in which LT10 and/or LT11 were blocked showed weaker steering responses (Fig. 1C) to all types of motion stimuli tested compared with their controls (supplementary material Fig. S1A). The other two blocking strains were similar (data not shown).

To further compare response amplitude between stimuli and strains, the mean peak-to-peak amplitude of each average trace over the entire trace duration was calculated (denoted as R). The relative mean amplitude for each stimulus/genotype pair tested was defined as R/R_{max}, where R_{max} is the single largest value of R across all stimulus/genotype pairs. These data appeared to reveal considerable variation in even control strains to different stimuli (supplementary material Fig. S1B), which may be caused by the disparate genetic

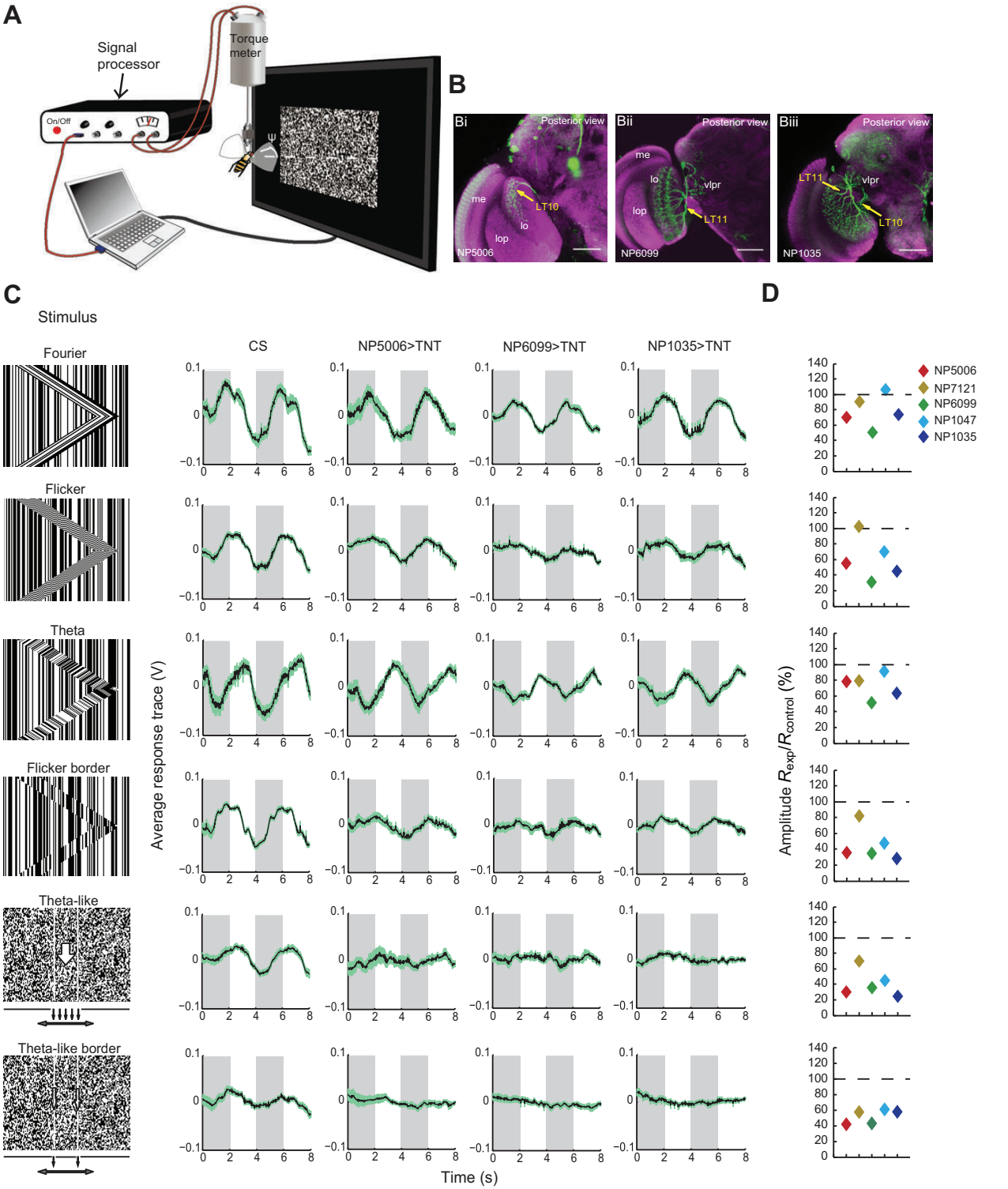

Fig. 1. Optomotor response traces to six types of motion stimuli. (A) Schematic diagram of experimental setup. The stimulus image spans ψ=142 deg in azimuth as seen by the fly. (B) Arborization patterns of the visual projection neurons LT10 and LT11. Bi–iii: Gal4-driven green fluorescent protein (GFP) expression in LT10 and LT11 in three strains. The Gal4 driver number is indicated in the bottom-left corner of each panel. The GFP signal (green) and the specimen labeled by anti-nc82 antibody (magenta) were excited at 488 and 561 nm, respectively, using a confocal microscope. me, medulla; lo, lobula; lop, lobula plate; vlpr, ventral lateral protocerebrum. Scale bars, 50 µm. (C) Optomotor response traces to each type of motion stimulus. The six panels of the leftmost column show space–time plots of one cycle of six types of stimuli, illustrating how one row (top row) chosen from the stimulus image at one instant of time evolves with time (vertical axis). The reverse dot speed within the theta object is the same as the theta bar speed. The next four columns display the corresponding optomotor responses to each stimulus in flies whose strain is marked at the top of each column, shown by the average response traces in black flanked by the standard error in green. Only the first two cycles of each average trace were plotted for clarity. (D) Percentage of the response amplitude in each blocking line (R_{exp}) relative to that in its heterozygous Gal4 control ($R_{control}$) for each stimulus tested. A general decrease in response amplitude occurred in almost all experimental groups irrespective of stimulus type. Ten to 25 flies were used for each data point in C and D.

backgrounds of the Gal4 lines, though the backgrounds of these NP series were only different in the X chromosome (Yoshihara and Ito, 2000). By calculating the percentage of the response amplitude in each blocking line relative to that in its heterozygous Gal4 control for each stimulus tested, it was found that a widespread reduction in R/R_{max} occurred in nearly all experimental groups regardless of stimulus type (Fig. 1D).

Within-genotype variability in response amplitude was examined by performing single-fly steering trace-based analysis (supplementary material Table S1). The mean peak-to-peak amplitude of each single-fly trace over the entire trace duration was calculated (denoted as R_{single}), and the mean amplitude $\bar{R}_{single}$ of individual flies for each stimulus/genotype pair tested is summarized in supplementary material Table S1. A one-way ANOVA with Bonferroni correction for multiple comparisons confirmed the results in Fig. 1D: blocking the two VPNs induced a general reduction in the mean response amplitude $\bar{R}_{single}$ of individual flies under most experimental conditions. Moreover, a strain-type-dependent reduction in response amplitude was obvious (Fig. 1D, supplementary material Table S1). For example, the response amplitude was seldom decreased in the NP7121>TNT line, whereas a considerable decrease always appeared in NP1035>TNT to almost all stimuli (Fig. 1D, supplementary material Table S1). These differences might be due to the different efficiencies of expression of Gal4 lines. It is worth noting that for theta-like border motion, the mean response amplitude of individual flies in experimental groups showed no significant reduction compared with their controls (supplementary material Table S1). More detailed analysis of the steering responses to theta-like border stimuli will be provided below.

Blocking lobula-specific VPNs LT10 and LT11 lengthens response delay only to MDSM

In addition to uniformly decreasing fly response amplitude to almost all of the motion stimuli tested, silencing the two VPNs by expressing tetanus toxin might also affect the shape and timing of the tracking responses. We therefore calculated the cross-correlation between the response traces and the time course of the bar position with a frequency of 0.25 Hz. Under open-loop test conditions as used in our experiments, flies displaying weaker tracking amplitudes should exhibit a highly coherent but tiny response signal if motion perception was intact.

Using a method similar to that described by Theobald et al. (Theobald et al., 2010), the MCC and the corresponding time lag were obtained based on average trace-based analysis (see Materials and methods). The MCC index has a range of [–1, 1], evaluating the extent to which a fly tracks a moving feature, no matter how weak the fly's response is. The time lag index quantifies tracking or response delay. The smaller the time lag, the shorter the lag between the movement of the stimulus and the reaction of the fly. In the case of the CS strain, for instance, the response to Fourier and flicker-defined second-order motion was almost immediate; however, the response to theta motion had a longer delay (~920 ms). By further altering the dot speed inside the theta bar, the response delay was found to be a function of the ratio of internal dot speed to speed of the bar itself, as shown in Fig. 2. This result is in agreement with those from previous studies on theta motion in CS flies (Theobald et al., 2008; Theobald et al., 2010), indicating that our experimental setup using a flat LCD works as well as a cylindrical screen for investigating motion tracking, on the condition that the motion stimuli were slow enough to be clearly seen on the LCD.

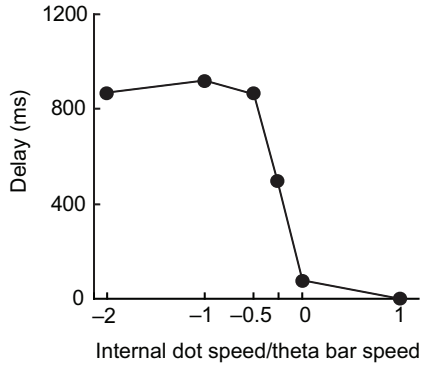

Fig. 2. Response delay in CS flies to theta motion with different internal dot speeds. The ratio of internal dot speed to theta bar speed is indicated on the *x*-axis. The ratios +1.0 and 0 correspond to Fourier and flicker border motion, respectively. Data points are the lags of average optomotor traces, all of which have the corresponding MCC indices larger than 0.82. Twelve to 21 CS flies were used for each data point.

The MCC and lag of the average traces under each experimental condition are shown in Fig. 3A,B. All blocking lines showed a high MCC index to all the stimuli except the theta-like border motion, although the MCC index in the blocking lines to theta-like motion was slightly attenuated. The very low MCC under the theta-like border stimulus condition (Fig. 3A) indicated that the tracking responses in the blocking lines were seriously impaired and therefore that the response delays to this stimulus were not tenable. This result, together with the mean response amplitude data shown in supplementary material Table S1, suggested that the abolished tracking responses to theta-like border motion (Fig. 1C) were not due to the weak responses, rather the blocking lines did not robustly follow this stimulus.

By examining the lags for all tracking responses except those to theta-like border motion, all blocking lines were found to show quite retarded responses to theta and theta-like motion in comparison with their controls, whereas there seemed to be no coherent difference between the experimental and control groups in the case of Fourier and flicker-defined stimuli (Fig. 3B). Although the response amplitudes to almost all of the stimuli were generally influenced by blocking the two VPNs (Fig. 1C,D, supplementary material Fig. S1), it appeared that response delays only to MDSM were affected by blocking these neurons.

The above cross-correlation analysis is based on the average traces and thus helps mitigate the between-trial variation to which the lag index calculation is highly sensitive (Theobald et al., 2010). To investigate within-genotype variability in the lag index and statistically compare the experimental groups with their controls, we further performed single-fly steering trace-based analysis (Fig. 3C). The MCC and lag of each single-fly response trace were calculated using the same method as that used for the average traces. A few flies whose time lag was meaningless in cases where the MCC index was below chance level were excluded from analysis. To determine the chance level, non-periodic random stimuli, in which dots from the random-dot background jumped around erratically, were presented to the CS flies, and the upper bound of the 95% confidence interval of the MCC distribution was found to be 0.22 (N=15). The lags of single-fly traces with an MCC index not less than 0.27 for each stimulus/genotype pair tested were found to be normally distributed. Therefore, the flies showing MCC indices ≥0.27 were qualified for statistical analysis (Fig. 3C). It is worth

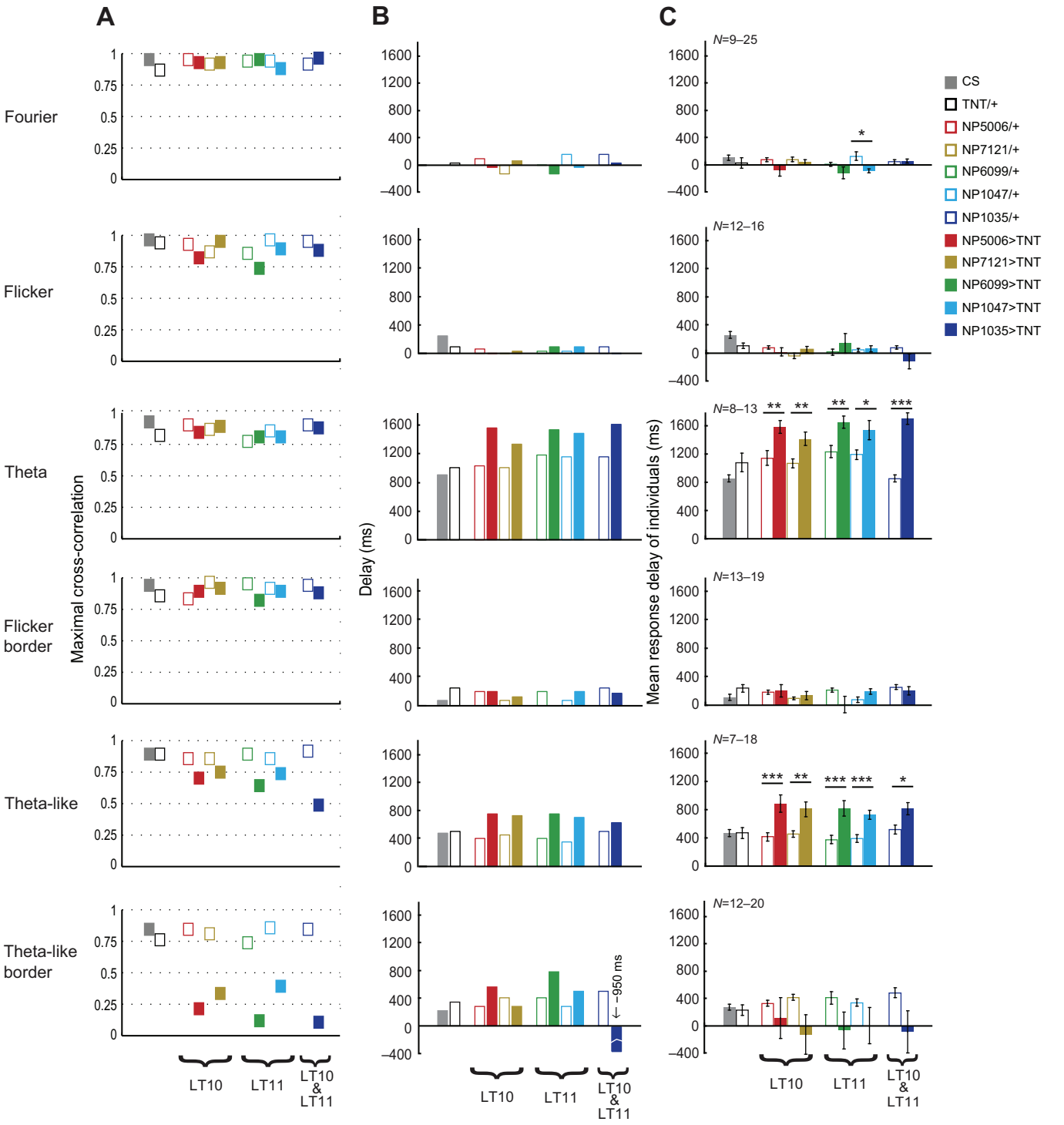

Fig. 3. The influence of blocking lobula-specific VPNs LT10 and/or LT11 on the response lag and maximal cross-correlation coefficient (MCC) indices. (A) The MCC indices of average optomotor traces under various experimental conditions shown in Fig. 1C are summarized here. The MCC index was found to be high enough to evidence robust tracking responses in all conditions but those in the blocking lines to theta-like border motion. The very low MCC index in the blocking lines to theta-like border stimulus indicated that their tracking responses were seriously impaired. (B) The response delays corresponding to A. Response delays to theta and theta-like motion stimuli were consistently lengthened in five Gal4-driven TNT strains compared with those measured in the heterozygous Gal4 driver controls. By contrast, the response delays to Fourier, flicker bar and flicker border stimuli in the blocking lines were of a similar level to their control lines. The delays of the experimental groups to the theta-like border stimulus were not tenable due to their very low MCC index. Ten to 25 flies were used for each data point in A and B. (C) The mean response delays of individual flies with the s.e.m. for each strain and stimulus tested (N=7–25). The delays of the experimental groups to theta-like border motion have no meaning due to a very low corresponding MCC index (see Results), for which statistical comparison is not applicable (these mean lags are still shown here for visual inspection). Student's t-test analysis revealed significant differences in the lag index between each blocking line and the corresponding control under theta and theta-like stimuli, whereas there were almost no significant differences for the cases of Fourier and flicker-defined motion conditions. *P≤0.05; **P≤0.01; ***P≤0.001.

noting that this MCC threshold (0.27) is slightly larger than the MCC value (0.22) to non-periodic random stimuli, which may be caused by between-sample variation. Student's *t*-test analysis showed that all the experimental groups displayed significantly longer delays than their heterozygous Gal4 controls under theta and theta-like stimuli, whereas there was almost no significant difference found for the cases of Fourier and flicker-defined motion (Fig. 3C). The NP1047>TNT line showed a significantly shorter delay than its control under Fourier stimulus (P=0.011; Fig. 3C), but other experimental groups were not significantly different from their controls under the same stimulus. Thus, the results did not support the hypothesis that blocking LT10 and/or LT11 would affect the response delays to Fourier motion. Taken together, these results showed that blocking LT10 or LT11 activity impacted the tracking response delay to MDSM, but not to non-MDSM signals.

The lags in all neuron blocking lines to the theta-like border motion (Fig. 3C) were meaningless, because their corresponding MCC index was too low. Specifically, the mean (±s.e.m.) MCC values of flies were 0.16±0.02, 0.22±0.04, 0.15±0.02, 0.21±0.02 and 0.14±0.01 for NP5006>TNT, NP7121>TNT, NP6099>TNT, NP1047>TNT and NP1035>TNT, respectively. These lags in each blocking line passed the uniform rather than normal distribution test. These results indicate that blocking the two VPNs impaired the ability of flies to track the theta-like border motion, which is consistent with the average trace-based analysis shown in Fig. 3A,B.

The specific effect of the LT10 and/or LT11 blocking on the tracking response delays to the MDSM stimuli should not arise from the dynamic characteristics within the moving figure, because no effect was observed on non-MDSM stimuli, irrespective of whether the moving figure had a dynamically flickering surface (flicker type) or was static (flicker border type) (Fig. 3B,C). Our results suggest that LT10 and/or LT11 are involved in detecting second-order stimuli defined by local motion but not flicker modulation. And the involvement is independent of whether the second-order feature is moving perpendicular or opposite to the local first-order motion. The hypothesis implies that flies in which LT10 and/or LT11 are blocked should have difficulty in perceiving a figure only defined by an MDSM border. This deduction was confirmed by our results under theta-like border stimuli, as explained above.

To probe whether the lengthened response delay to theta-like motion was caused by a weakened sensitivity to vertical movement, optomotor responses were tested in three blocking lines by utilizing a pure first-order motion in the vertical direction. The stimulus was similar to the theta-like motion except that the position of the theta-like object always remained stationary (supplementary material Fig. S2B). The torque meter, not suitable for recording behavior in pitch, was replaced by a pair of stereo microphone recorders. The sound wave amplitude of each wing vibration was measured by an AFS in real-time, which was transferred into the WBS traces of the left and right wings (see Materials and methods). To test whether the AFS functioned properly, we first examined the optomotor responses in the CS flies to horizontal Fourier stimulus. The turning behavior in yaw was measured using the torque meter and microphones simultaneously. It was shown that the L–R WBS signal was proportional to the yaw torque measured by the torque meter (supplementary material Fig. S2A), indicating that the method of measuring the sound wave of wing vibration was workable. The AFS was then used alone to test the fly's optomotor behavior in pitch and possible lift response. For a stimulus moving down and up, the L+R WBS signal decreased and increased, respectively. Thus the recorded signal is positively correlated with the stimulus direction and reports the pitch and lift responses (supplementary material Fig. S2C). Results showed that the optomotor responses in the CS and blocking lines (supplementary material Fig. S2C) expressed quite high MCC values and short delays (supplementary material Fig. S2D), indicating that flies in which LT10 and/or LT11 were blocked were able to perceive stimuli moving up or down.

Blocking lobula-specific VPNs LT10 and LT11 reduces response sensitivity to the salience modulation of theta motion

The above results indicate the involvement of the VPNs LT10 and LT11 in MDSM perception. Because MDSM contains first- and second-order components, we speculate that the two VPNs may play a role in the interaction between the two motion detection systems. To test this idea, the above experiments were repeated but the salience of the theta stimulus was changed by altering the internal dot speed. The mean response delay of individual flies in nearly all blocking lines showed significantly retarded responses in comparison with their controls (Fig. 4A, left column). This result was consistent with that obtained under standard theta stimuli (Fig. 3C), supporting the hypothesis that blocking two pathways, LT10 and LT11, lengthens the response delay to MDSM.

In order to investigate whether and how the relationship between the internal motion speed and tracking delay (as shown in Fig. 2) was affected by blocking the two VPNs, the average trace-based cross-correlation analysis was further examined. A high MCC index indicated that robust optomotor responses persisted in both blocking and control lines under all three kinds of internal speed used, although the MCC in the blocking lines was slightly lowered when the speed was very low (internal dot speed/theta bar speed=–0.25; Fig. 4A, right column). The response lag was modulated by manipulation of the salience of the theta bar (Fig. 4A, bottom panels). Because the dependence of the response delays on the internal speed was not highly linear in most strains, the maximal change of the response delay, rather than the linear regression analysis, was examined. By modulating the internal speed within the range –0.25 to –2.0, the maximal change of the response delay for each strain was calculated and labeled for easy comparison (Fig. 4A, bottom panels). Results showed that most control lines (four-fifths) were affected by the salience manipulation of the theta bar more strongly than the blocking lines (Fig. 4A, bottom panels).

When we investigated the response amplitude of the average response traces, both the blocking lines and their controls showed sensitivity to the speed of internal dots (Fig. 4B, top panels). However, linear regression analysis revealed that the rate of amplitude rise was apparently slower in four-fifths of the blocking lines than in their controls when the internal speed was increased from –0.25 to –2.0 (Fig. 4B, bottom panels). A reduction in sensitivity to the salience of second-order motion cues in LT10- and/or LT11-blocked flies was consistently observed in both the response lag and amplitude. These results may reflect an impairment of the modulation role played by the two VPN pathways, when the competition dominance was changed between the first- and second-order motion processing systems. Our speculation is supported by the attenuated MCC index in both theta-like and theta-like border motion conditions lacking a Fourier motion component in the horizontal direction (Fig. 3A). The more severely reduced MCC in the case of theta-like border motion may be a consequence of a sharp decline in the relative salience of the second-order motion cues.

A decrease in response amplitude in the CS flies has been observed previously in cases where the speed ratio was changed from +1.0 to –1.0 [fig. 5B in Theobald et al. (Theobald et al., 2010)].

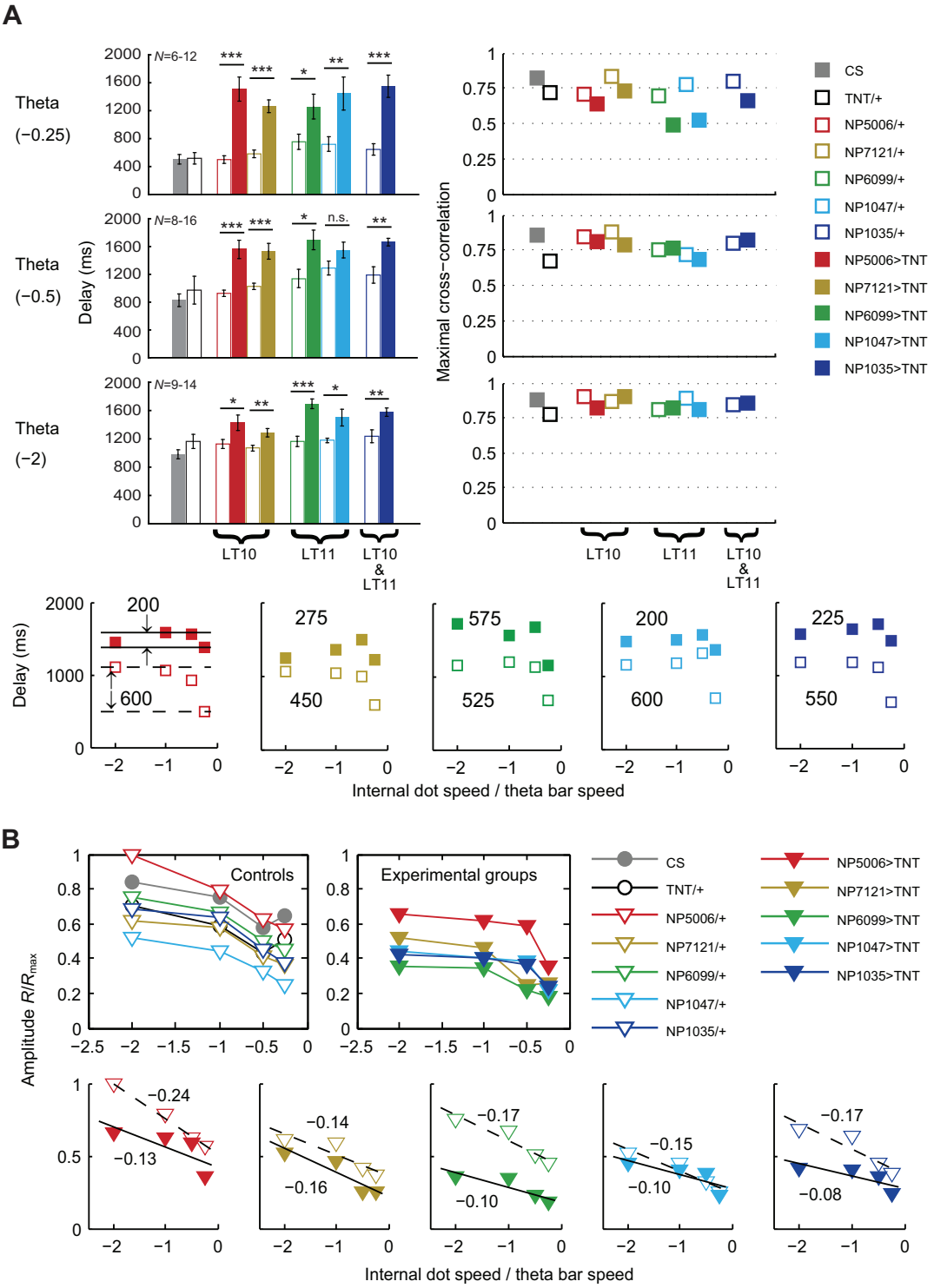

Fig. 4. Effect of the salience modulation of theta motion on optomotor responses. (A) The mean ± s.e.m. response delays of 6–16 flies (left panels), the MCC index of the average optomotor traces (right panels) and the dependence of the lag index of the average optomotor traces on the internal dot speed (bottom panels). Within the whole range of the internal speed tested, the induced maximal change in the response delay for each strain was calculated and labeled, as illustrated by the distance between two dashed (heterozygous Gal4 control) or solid (blocking line) parallel lines in the bottom leftmost panel. In each panel the upper and lower numbers are the induced maximal change in the response delay for the blocking line and its heterozygous Gal4 control, respectively. The change in response delay was less sensitive to the internal speed in LT10 and/or LT11 blocked lines than in their controls (bottom panels). (B) The dependence of the relative mean amplitude R/R_{max} of the average optomotor traces on the internal dot speed (top panels) and linear regression analysis (bottom panels). The straight regression lines (R^2=0.57 to 0.99) are illustrated by dashed lines for the control groups and solid lines for the experimental groups, and their slopes are also labeled for easy comparison (bottom panels). The response amplitude increases monotonically with the reverse dot speed inside the theta bar in LT10 and/or LT11 blocking lines (right panel) at a slower rate of increase than in most controls (four-fifths) (left panel). Ten to 16 flies were used for each data point except three top left panels of A with the fly number indicated. *P≤0.05; **P≤0.01; ***P≤0.001 (Student's t-test).

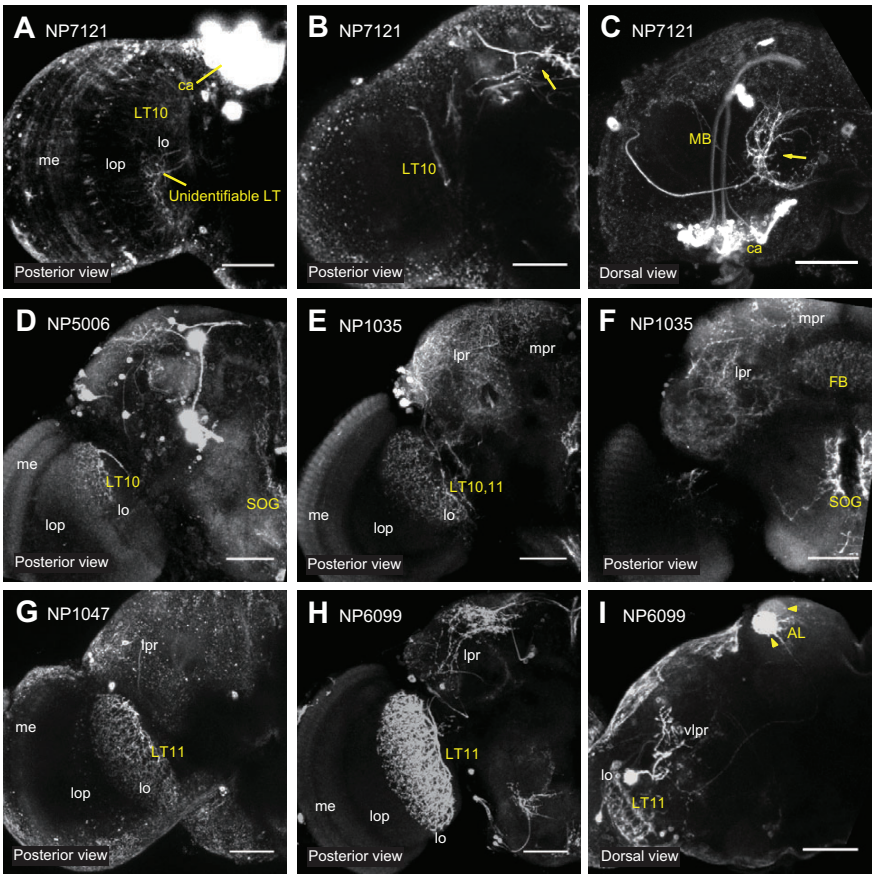

Fig. 5. Expression pattern of the five Gal4 strains. Serial sections from posterior (A,B,D–F,G,H) and dorsal (C,I) viewing angles were superimposed to display the labeled cells. Images of the same line were of different sections superimposed for clarity. The Gal4 driver number is indicated in the top left corner. The neuron showing the detailed arborization and marked by the yellow arrows in B and C was the same cell. Two glomeruli of the antennal lobe labeled are indicated by the yellow arrowheads in I. me, medulla; lo, lobula; lop, lobula plate; lpr, lateral protocerebrum; mpr, medial protocerebrum; ca, calyx; unidentifiable LT, lobula-specific tangential VPNs; MB, mushroom bodies; FB, fan-shaped body; SOG, suboesophageal ganglion; AL, antennal lobe. Scale bars, 50 μm.

Our result within the ratio range [+1.0, –0.5] qualitatively accords with theirs. When the speed ratio was changed from –0.5 to –2.0, the monotonically increasing function of speed shown in Fig. 4B seems opposite to that observed in Theobald et al. (Theobald et al., 2010). The discrepancy is probably due to a difference in the speed range used between the two studies. Moreover, such a discrepancy may be deceptive: the response amplitude appears to also have a minimum around the speed ratio of –0.6 in fig. 4B in Theobald et al. (Theobald et al., 2010). Due to the widespread influence of blocking LT10 and/or LT11 on the response amplitude irrespective of stimulus type, it is difficult in our study to analyze whether the tracking responses of the flies comply with Theobald et al.'s hypothesis on the linear superposition of first- and second-order components (Theobald et al., 2010; Aptekar et al., 2012).

DISCUSSION

Expression patterns of the five Gal4 lines hardly overlap in regions other than the LT10 and LT11

The LT10 and LT11 neurons have been identified clearly by the Gal4 lines used in this study (Otsuna and Ito, 2006). Meanwhile, other parts of the optic lobes and the central brain were also labeled in these lines [fig. 16 in Otsuna and Ito (Otsuna and Ito, 2006)] (Fig. 5). In addition to the LT10, NP5006 labeled the suboesophageal ganglion and a few unidentified cells in the center brain (Fig. 5D), while NP7121 labeled unidentifiable lobula-specific tangential VPNs, medulla-specific tangential VPNs and some glial cells in the optic lobe (Otsuna and Ito, 2006) (Fig. 5A,B), as well as part of the mushroom bodies and other cells in the central brain (Fig. 5B,C). The expression pattern of NP1035 labeled the lateral and medial protocerebrum, the fan-shaped body and the suboesophageal ganglion (Fig. 5E,F). The lateral protocerebrum, but with different patterns and a few unidentified cells, was found labeled in NP1047 and NP6099, respectively (Fig. 5G,H). NP6099 also labeled a few glomeruli in each antennal lobe (Fig. 5I). These results, together with the images reported previously (Otsuna and Ito, 2006), show that except LT10 and LT11, these Gal4 lines rarely labeled the same region of the optic lobe and the central brain, supporting the hypothesis that the longer response delays to MDSM were caused by silencing the LT10 and LT11 rather than other cells labeled in the brain.

However, the potential influence of silencing other cells on MDSM perception may not be totally excluded. For example, the unidentifiable lobula-specific tangential VPNs (Fig. 5A) and the lateral protocerebrum were found labeled in some lines. These regions might also influence motion processing, as discussed below.

The increased response delay is the more specific phenotype produced by blocking LT10 and LT11

In addition to the central finding that blocking the synaptic output of several visual projection neurons from the lobula significantly lengthened the tracking response delay only to the MDSM, it was also found that such blocking generally decreased the response amplitude to all motion stimuli tested but did not affect the motion tracking fidelity (evidenced by the high MCC index). It is worth noting that single-fly steering trace-based analysis of the MCC, implicitly assumed to give a result consistent with the MCC based on the average traces, was not performed in our study because the signal-to-noise ratio of individual traces was considerably lower than that of the average trace, especially when the response magnitude was low. This problem may be solved by computing the MCC on the average response of each fly across multiple trials, but this solution was prohibited by our experimental design, which presented

each stimulus to each fly only once. However, it may be unnecessary to keep individual flies naive to the stimuli in future studies, as there is no evidence to support that the prior visual experience would influence the optomotor response in flies.

The general decrease in response amplitude might reflect some general changes induced by expressing tetanus toxin in the pathways for motion processing and/or motor control. In addition to the two lobula-specific VPNs, other cells throughout the brain were also targeted in each strain [fig. 16 in Otsuna and Ito (Otsuna and Ito, 2006)] (Fig. 5). Although the exact involvement of these labeled cells in motion-dependent behaviors is unknown, it is not surprising that expressing tetanus toxin in these cells leads to a general decrease of the response amplitude. Moreover, the response amplitude can be influenced by many factors, e.g. temperature, humidity or other environmental factors, as observed in our experiments and pointed out in Theobald et al. (Theobald et al., 2010). The response amplitude can also be influenced by physical strength and condition. The non-specific expression of tetanus toxin may cause some secondary effects on fertility, diet or locomotion, which would affect body size and physical condition *via* complicated organic mechanisms. Taken together, we thought that the increased response delay only to the MDSM is the more unequivocal and specific phenotype produced, rather than the decreased amplitude, by blocking these neurons.

An alternative hypothesis, that the LT10 and LT11 are involved in integrating motion signals over long time scales, also seems to be raised by the result that the response delay induced by the MDSM was longer than that induced by other types of stimuli (Figs 2, 3). The relatively long response delay may be caused by the processing of the conflicting motion signals in MDSM perception. Thus, other elaborately designed stimuli containing conflicting cues may be crucial for further understanding of the role of the lobula-specific VPNs in higher-order motion processing.

In summary, our results suggest that lobula-specific VPNs LT10 and LT11 may be not needed for Fourier and flicker-defined second-order motion detection but are indispensable for MDSM processing. Our results predict that other VPN pathways, not examined in this study, may be also involved in MDSM processing. Further in-depth analysis, at least for the 14 lobula-specific VPN pathways identified in *Drosophila* (Otsuna and Ito, 2006), is required to dissect the neural mechanisms underlying higher-order motion processing.

Lobula-specific VPNs may participate in the modulation of competition between two processing streams

MDSM contains two separate components: elementary motion (EM) and figure motion (FM) (Aptekar et al., 2012; Lee and Nordström, 2012). EM is confined within the figure and FM is the motion of the figure itself, which can be in a different direction from its internal EM. Theta motion can be viewed as a moving figure whose internal dots coherently move (EM) opposite to the direction of the figure itself (FM). Similarly, theta-like motion is a combination of EM and FM in two mutually perpendicular directions. Recent studies have argued that the tracking responses in flies to theta motion is the linear superposition of two separate motion-processing streams or two independent steering efforts towards EM and FM, respectively (Theobald et al., 2010; Aptekar et al., 2012). In our study, the lobula-specific VPN blocking was found not to affect the tracking delays to pure first-order Fourier (EM and FM have the coherent direction) or pure second-order Flicker-defined motion (only FM or FM plus flickering), whereas it did have influence over the response delays to the compound motion consisting of EM and FM in two opposite or perpendicular directions. The results suggest that the two lobula-specific VPN pathways are indispensible for the compound motion processing when its EM and FM are not coherent. Moreover, the weakened sensitivity to the speed modulation of EM component was observed in the compound motion perception by blocking the two VPNs (Fig. 4). This may reflect the modulation role of LT10 and LT11 pathways in the competition of the two processing streams for EM and FM.

A previous hypothesis suggests that there are separate or partially separate pathways for first- and second-order motion detection in mammals (Lu and Sperling, 1995; Baker, 1999; Rosenberg et al., 2010; Vaina and Cowey, 1996) and flies (Schnell et al., 2012). However, it seems that there exists no evidence of single neurons responding exclusively to second-order motion (Baker, 1999), although a large number of psychophysical results support the hypothesis. The neural computation necessary for extracting second-order motion signal is even sourced from the mammalian retina (Demb et al., 2001), though the visual cortex is commonly thought of as the place for detecting higher-order motion. Similarly, the neuronal basis for the hypothesis on separate motion pathways remains undetermined in flies. The H1 neuron, one of the lobula plate horizontal system cells in the blowfly, showed a preferred response to the direction of Fourier motion, flicker-defined motion, and the EM but not the second-order FM component of theta motion (Quenzer and Zanker, 1991). By contrast, electrophysiological recordings in hoverflies have recently disclosed significant responses in lobula plate tangential cells to theta motion (Lee and Nordström, 2012). And the ensemble of lobula output neurons, projecting to discrete optic glomeruli in the lateral protocerebrum, was found to respond to first-order motion in *Drosophila* (Okamura and Strausfeld, 2007; Mu et al., 2012). These results, including ours, suggest that first- and second-order motion processing is probably not dissociated, at least in the lobula plate, and their interaction or integration may happen in the lobula and the central brain.

LIST OF ABBREVIATIONS

AFS	acoustic flight simulator
CS	wild-type *Canton-S* strain
EM	elementary motion
FM	figure motion
MCC	maximal cross-correlation coefficient
MDSM	motion-defined second-order motion
VPN	visual projection neuron
WBP	wing beat processor
WBS	wing beat strength

ACKNOWLEDGEMENTS

We thank Dr Nicholas J. Strausfeld for valuable discussion.

FUNDING

This work was supported by the 973 Program [2011CBA00400 to A.G.] and the National Science Foundation of China [grant 30770495 to Z.W.; grants 30921064, 90820008 and 31130027 to A.G.].

REFERENCES

Aptekar, J. W., Shoemaker, P. A. and Frye, M. A. (2012). Figure tracking by flies is supported by parallel visual streams. *Curr. Biol.* **22**, 482-487.

Baker, C. L., Jr (1999). Central neural mechanisms for detecting second-order motion. *Curr. Opin. Neurobiol.* **9**, 461-466.

Borst, A. and Egelhaaf, M. (1989). Principles of visual motion detection. *Trends Neurosci.* **12**, 297-306.

Borst, A., Haag, J. and Reiff, D. F. (2010). Fly motion vision. *Annu. Rev. Neurosci.* **33**, 49-70.

Demb, J. B., Zaghloul, K. and Sterling, P. (2001). Cellular basis for the response to second-order motion cues in Y retinal ganglion cells. *Neuron* **32**, 711-721.

Douglass, J. K. and Strausfeld, N. J. (2003). Anatomical organization of retinotopic motion-sensitive pathways in the optic lobes of flies. *Microsc. Res. Tech.* **62**, 132-150.

Fischbach, K. F. and Dittrich, A. P. M. (1989). The optic lobe of *Drosophila melanogaster*. I. A Golgi analysis of wild-type structure. *Cell Tissue Res.* **258**, 441-475.
Götz, K. G. (1964). Optomotorische Untersuchung des visuellen Systems einiger Augenmutanten der Fruchtfliege *Drosophila*. *Kybernetik* **2**, 77-92.
Götz, K. G. (1987). Course-control, metabolism and wing interference during ultralong tethered flight in *Drosophila melanogaster*. *J. Exp. Biol.* **128**, 35-46.
Guo, A., Li, L., Xia, S. Z., Feng, C. H., Wolf, R. and Heisenberg, M. (1996). Conditioned visual flight orientation in *Drosophila*: dependence on age, practice, and diet. *Learn. Mem.* **3**, 49-59.
Heisenberg, M. and Wolf, R. (1979). On the fine structure of yaw torque in visual flight orientation of *Drosophila melanogaster*. *J. Comp. Physiol.* **130**, 113-130.
Joesch, M., Plett, J., Borst, A. and Reiff, D. F. (2008). Response properties of motion-sensitive visual interneurons in the lobula plate of *Drosophila melanogaster*. *Curr. Biol.* **18**, 368-374.
Lee, Y. J. and Nordström, K. (2012). Higher-order motion sensitivity in fly visual circuits. *Proc. Natl. Acad. Sci. USA* **109**, 8758-8763.
Lu, Z. L. and Sperling, G. (1995). The functional architecture of human visual motion perception. *Vision Res.* **35**, 2697-2722.
Mu, L., Ito, K., Bacon, J. P. and Strausfeld, N. J. (2012). Optic glomeruli and their inputs in *Drosophila* share an organizational ground pattern with the antennal lobes. *J. Neurosci.* **32**, 6061-6071.
Okamura, J. Y. and Strausfeld, N. J. (2007). Visual system of calliphorid flies: motion- and orientation-sensitive visual interneurons supplying dorsal optic glomeruli. *J. Comp. Neurol.* **500**, 189-208.
Orger, M. B., Smear, M. C., Anstis, S. M. and Baier, H. (2000). Perception of Fourier and non-Fourier motion by larval zebrafish. *Nat. Neurosci.* **3**, 1128-1133.
Otsuna, H. and Ito, K. (2006). Systematic analysis of the visual projection neurons of *Drosophila melanogaster*. I. Lobula-specific pathways. *J. Comp. Neurol.* **497**, 928-958.
Quenzer, T. and Zanker, J. M. (1991). Visual detection of paradoxical motion in flies. *J. Comp. Physiol. A* **169**, 331-340.
Roeser, T. and Baier, H. (2003). Visuomotor behaviors in larval zebrafish after GFP-guided laser ablation of the optic tectum. *J. Neurosci.* **23**, 3726-3734.
Rosenberg, A. and Issa, N. P. (2011). The Y cell visual pathway implements a demodulating nonlinearity. *Neuron* **71**, 348-361.
Rosenberg, A., Husson, T. R. and Issa, N. P. (2010). Subcortical representation of non-Fourier image features. *J. Neurosci.* **30**, 1985-1993.
Schnell, B., Raghu, S. V., Nern, A. and Borst, A. (2012). Columnar cells necessary for motion responses of wide-field visual interneurons in *Drosophila*. *J. Comp. Physiol. A* **198**, 389-395.
Strausfeld, N. J. (1991). Structural organization of male-specific visual neurons in calliphorid optic lobes. *J. Comp. Physiol. A* **169**, 379-393.
Sweeney, S. T., Broadie, K., Keane, J., Niemann, H. and O'Kane, C. J. (1995). Targeted expression of tetanus toxin light chain in Drosophila specifically eliminates synaptic transmission and causes behavioral defects. *Neuron* **14**, 341-351.
Tammero, L. F., Frye, M. A. and Dickinson, M. H. (2004). Spatial organization of visuomotor reflexes in *Drosophila*. *J. Exp. Biol.* **207**, 113-122.
Theobald, J. C., Duistermars, B. J., Ringach, D. L. and Frye, M. A. (2008). Flies see second-order motion. *Curr. Biol.* **18**, R464-R465.
Theobald, J. C., Shoemaker, P. A., Ringach, D. L. and Frye, M. A. (2010). Theta motion processing in fruit flies. *Front. Behav. Neurosci.* **4**, 35.
Vaina, L. M. and Cowey, A. (1996). Impairment of the perception of second order motion but not first order motion in a patient with unilateral focal brain damage. *Proc. R. Soc. B* **263**, 1225-1232.
Yoshihara, M. and Ito, K. (2000). Improved Gal4 screening kit for large-scale generation of enhancer-trap strains. *Drosoph. Inf. Serv.* **83**, 199-202.